Solution of a model of self-avoiding walks with multiple monomers per site on the Husimi lattice

Tiago J. Oliveira* and Jürgen F. Stilck†
Instituto de Física, Universidade Federal Fluminense, Avenida Litorânea s/n, 24210-346-Niterói, Rio de Janeiro, Brazil

Pablo Serra‡
Facultad de Matemática, Astronomía y Física, Universidad Nacional de Córdoba, Córdoba-RA5000, Argentina
(Received 16 February 2008; published 4 April 2008)

We solve a model of self-avoiding walks which allows for a site to be visited up to two times by the walk on the Husimi lattice. This model is inspired in the Domb-Joyce model and was proposed to describe the collapse transition of polymers with one-site interactions only. We consider the version in which immediate self-reversals of the walk are forbidden. The phase diagram we obtain for the grand-canonical version of the model is similar to the one found in the solution of the Bethe lattice, with two distinct polymerized phases: a tricritical point and a critical endpoint.

DOI: 10.1103/PhysRevE.77.041103 PACS number(s): 05.40.Fb, 05.70.Fh, 61.41.+e

I. INTRODUCTION

Although linear polymers in solution may be studied using continuous models, much has been learned about these systems through models of self-avoiding and mutually avoiding walks placed on lattices [1]. The excluded-volume constraint makes it quite difficult to treat these problems; even trying to answer apparently simple questions such as the number of walks with a given number of steps, which is relevant in series expansion approaches to the problem, is a challenging and rich field of research (for a recent work in this field see [2]). The connection of such models with the n-vector model of magnetism in the formal limit $n \to 0$ [3] and the application of the ideas of scaling and the renormalization group to polymer systems [4] have also been central in the development of this area of research.

If the polymer chain is placed in a poor solvent, as the temperature is decreased eventually the chain changes from an extended configuration (in which the entropy is favored) to a collapsed configuration (with less contact between the polymer and the solvent and thus a smaller energy). The temperature where this transition happens is called the θ temperature [1]. Although this transition may be modeled using lattice models where the solvent is included explicitly [5], these models in a certain limit lead to a simpler model which has become the standard model for this phenomenon, in which, besides the repulsive excluded-volume interactions, attractive interactions between monomers on first neighbor sites but not consecutive along the chain are introduced (ISAW model). The configurations in this model are self-avoiding walks whose steps link monomers located on first-neighbor lattice sites. The collapse transition in models which are grand canonical with respect to the number of monomers in the system usually appears as a tricritical point in the phase diagram. In the fugacity versus temperature phase diagram, a nonpolymerized phase is present in the region of low monomer fugacity and a polymerized phase is stable for higher fugacities. The transition between these phases is of first order at low temperatures and becomes continuous at higher temperatures. These regimes are separated by a tricritical point, where the collapse transition occurs. The ISAW model has been extensively studied on the square lattice [6], and the exact tricritical exponents of the diluted polymer model were found [7]. Under certain conditions, an even richer phase diagram is found, with the presence of a dense polymerized phase at finite monomer fugacity, where the density of empty lattice sites vanishes. This additional phase was found in solutions of the model on $q=4$ Husimi lattices with interactions between *bonds* [8,9] of the polymer located on opposite sides of elementary squares of the lattice, as well as in cluster approximations of similar models on the square lattice [10]. Transfer matrix calculations on strips of finite widths support the existence of this phase on the square lattice as well [11]. The dense phase is absent if the interactions are only between monomers, but even in this case there are indications that this phase will be present if the polymer chains are sufficiently stiff [12].

Usually, the introduction of interactions in the polymer models is a source of difficulty both in approximate solutions and in transfer-matrix approaches. Thus, a model introduced recently for studying the collapse transition in polymers where only *one-site* interactions are present is quite interesting [13]. This model allows for multiple occupancy of a site by up to K monomers, assuming that the attractive interactions are restricted to monomers which occupy the same site of the lattice. One way to justify the model would be to discretize the original system of a polymer in a solution using a regular lattice and choosing the size of the elementary cell of this lattice to be large enough to accommodate up to K monomers of the polymer. Also, the length of the bonds has to be larger than the size of the cells, so that two monomers in the same cell will never be connected by a bond. Two versions of the model were studied by extensive numerical simulations in [13] on the square and on the cubic lattice. In the RA (immediate reversals allowed) model, there are no restrictions on the walks on the lattice, while in the RF (immediate reversals forbidden) model only a subset of the possible walks is considered: those in which the walk does

*tiagojo@if.uff.br
†jstilck@if.uff.br
‡serra@famaf.unc.edu.ar

not return to the original site immediately after reaching a new site. In the simulations done for the RF model on the cubic lattice for $K=3$, a transition between extended and collapsed polymerized phases is found.

Recently, the RA and RF models were solved on a Bethe lattice for $K=2$, in order to compare their thermodynamic behaviors with the much studied ISAW model regarding the usual collapse transition [14]. The solution of the RF model on the Bethe lattice produces a phase diagram in which the polymerization transition remains continuous for small nonzero values of ω_2, becoming of first order at higher values of this statistical weight, a behavior which is also found in the ISAW model. Besides the regular polymerized phase, a second phase is stable for sufficiently high values of ω_2 and low values of ω_1 where only empty and double-occupied sites are present.

Here the RF model is solved on a $q=2(\sigma+1)$ Husimi lattice, which is the central region of a Cayley tree built with squares. There are $\sigma+1$ squares incident on each lattice site. The thermodynamic behavior of models on such a lattice is expected to be closer to the one obtained on a regular lattice with the same coordination number, and we were motivated for this calculation mainly for two reasons. Although the RF model on the Bethe lattice displays a tricritical point which may be associated with the usual collapse transition of polymers, if we parametrize the model such that $\omega_1=z$, the activity of a monomer, and $\omega_2=z^2\omega$, where ω is the Boltzmann factor associated with a pair of interacting monomers, the tricritical point is found at $\omega<1$, a value that corresponds to a *repulsive* interaction between monomers at the same site. We are interested in finding out if a calculation which should lead to results closer to the ones on regular lattices might shift the tricritical point to the region in the parameter space which corresponds to attractive interactions. Also, it is of interest to find out if the second polymerized phase is still present in the phase diagram of the model on the Husimi lattice. We found that actually with a convenient parametrization the tricritical point is located in the physically expected region and that the second polymerized phase is still present in the Husimi lattice solution, although it occupies a smaller region of the parameter space than the one found for the Bethe lattice.

In Sec. II we define the model in more detail and present its solution on the Husimi lattice. Final discussions and the conclusion may be found in Sec. III.

II. DEFINITION OF THE MODEL AND SOLUTION ON THE HUSIMI LATTICE

We consider a Husimi tree, a Cayley tree built with polygons, which in our case will be squares. Sometimes this tree is also called a cactus. As also happens for the Cayley tree, in the thermodynamic limit the fraction of sites which are on the surface of the tree does not vanish and this accounts for the fact that the solution of models on such trees usually shows a behavior which does not resemble the one found on regular lattices. If, however, the behavior of models in the central region of the trees is considered, for many models the exact solution corresponds to the Bethe approximation of the same model on a regular lattice with the same coordination number and this is the reason why this is called a Bethe lattice solution [15]. The Husimi lattice corresponds to the central region of a Cayley tree built with polygons (squares in our case), and since closed paths are present (although restricted to single elementary squares), it is expected that the solution of models on this tree will be closer to the one found on regular lattices and this is confirmed in many cases.

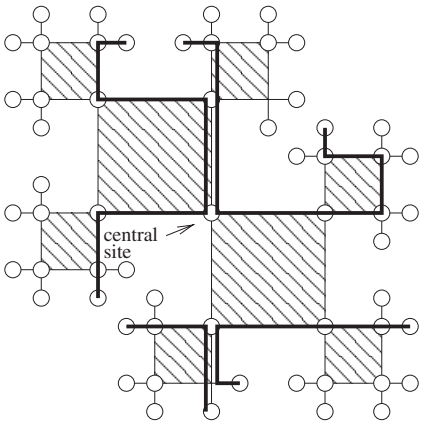

FIG. 1. Example of a configuration for the $K=2$ RF model on a Husimi tree with square ramification $\sigma=1$ and 2 generations. Polymer bonds (steps of the walks) are represented by thick lines, while the lattice bonds are thin lines. The weight of this configuration is $\omega_1^{12}\omega_2^4$.

The allowed configurations of the $K=2$ RF model are walks that may visit a site one or two times, with their initial and final monomers placed only on the surface of the tree. Also, as stated above, immediate reversals of the walk are forbidden. In Fig. 1 a possible configuration is shown on a tree with two generations of squares. The statistical weight of a configuration will be $\omega_1^{N_1}\omega_2^{N_2}$, where N_1 and N_2 are the numbers of sites with one and two monomers, respectively. For simplicity, the surface of the tree was chosen to be defined by sites connected to a single site of the first generation of squares. To solve the model on the Husimi tree, we consider rooted subtrees and define partial partition functions for these trees for fixed configurations of the bonds incident on the root site. The operation of attaching three sets of σ n-generation subtrees to a new root square will result in a $(n+1)$-generation subtree, leading to recursion relations for the partial partition functions. Notice that we decided to consider the monomers placed on the same site to be *indistinguishable*, in opposition to what was adopted in the solution on the Bethe lattice [14], where they were supposed to be distinguishable. This convention was motivated mainly by two aspects: as already observed in the discussion of the Bethe lattice solution, the tricritical point of the $K=2$ RF model is located in the region in the parameter space which corresponds to *repulsive* interactions between monomers. If two monomers placed on the same site are considered to be indistinguishable, the weight ω_2 will be multiplied by a factor of 2 and this will shift the tricritical point toward the region of attractive monomers. Also, in the original simulations [13] the configurations of a walk on the lattice are labeled by the sequence of sites visited by the walk and this

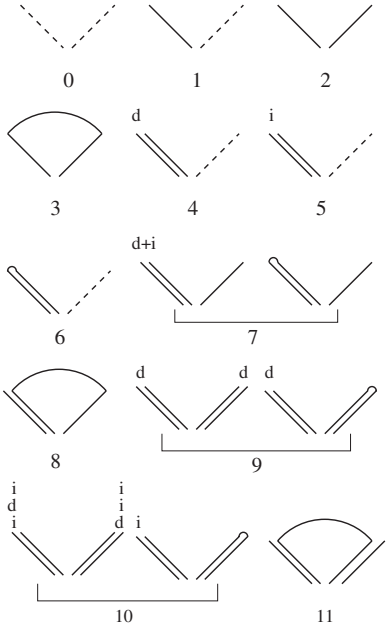

FIG. 2. Root configurations of the RF model with $K=2$ on the Husimi lattice.

convention corresponds to indistinguishable monomers. Although we do no detailed comparisons of our results with the simulations, since they were done for $K=3$, we decided to adopt the same convention. In Fig. 2 the 11 configurations of the bonds incident on the root site of subtrees are depicted. For brevity, only one configuration of pairs related by reflection symmetry is shown. For example, there are a total of four configurations with the same partial partition function in group 7 of the figure. We notice that the connection of the incoming bonds to the monomers placed on the root site is not fixed. Since we assume the monomers to be indistinguishable, to write down the recursion relations for the partial partition functions we must separate incoming double bonds into two groups: if both bonds visited the same sites since the boundary of the tree they are labeled as i (as in configuration 5); otherwise, they are labeled as d (as in configuration 4). This information is essential to allow us to correctly determine the multiplicity of the contributions to the recursion relations below.

We may now proceed obtaining the recursion relations for the partial partition functions. We notice that certain partial partition functions appear in the recursion relations only in linear combinations. Thus, g_3 and g_6 always appear as g_3+g_6 and the other linear combinations are $2g_7+g_8$ and $2g_9+g_{11}$. We therefore may reduce the number of independent variables in the recursion relations by 3. The partial partition functions usually diverge in the thermodynamic limit; thus, we consider the eight ratios defined below, which often remain finite, and in the thermodynamic limit a phase of the system may be associated with a fixed point of the recursion relations for the ratios:

$$R_1 = \frac{g_1}{g_0}, \tag{1a}$$

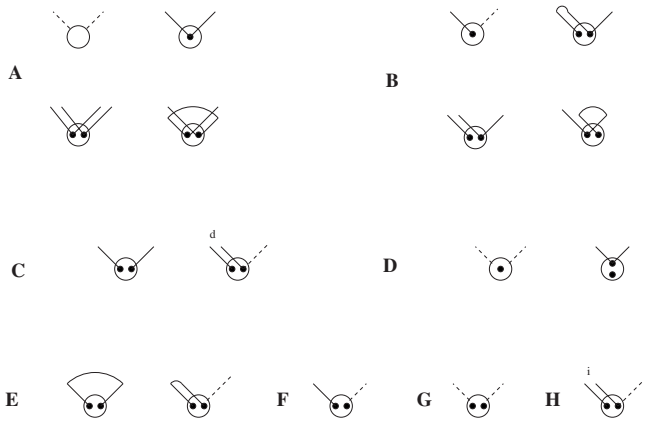

FIG. 3. Contributions to the vertex functions. The monomers are represented by dots.

$$R_2 = \frac{g_2}{g_0}, \tag{1b}$$

$$R_3 = \frac{g_3 + g_6}{g_0}, \tag{1c}$$

$$R_4 = \frac{g_4}{g_0}, \tag{1d}$$

$$R_5 = \frac{2g_7 + g_8}{g_0}, \tag{1e}$$

$$R_6 = \frac{2g_9 + g_{11}}{g_0}, \tag{1f}$$

$$R_7 = \frac{g_5}{g_0}, \tag{1g}$$

$$R_8 = \frac{g_{10}}{g_0}. \tag{1h}$$

It is now convenient to define first some linear combinations of partial partition functions which appear repeatedly in the recursion relations, whose contributions are shown graphically in Fig. 3 for the particular ramification of squares $\sigma=1$. They are

$$\begin{aligned} A = g_0^{\sigma}\Bigg[& 1 + \sigma\omega_1 R_2 + \binom{\sigma}{2}\omega_1 R_1^2 + \sigma\omega_2 R_6 + \sigma\omega_2 R_8 \\ & + 2\binom{\sigma}{2}\omega_2 R_4^2 + 2\binom{\sigma}{2}\omega_2 R_4 R_7 + \binom{\sigma}{2}\omega_2 R_7^2 \\ & + 4\binom{\sigma}{2}\omega_2 R_3 R_4 + 2\binom{\sigma}{2}\omega_2 R_3 R_7 + 4\binom{\sigma}{2}\omega_2 R_2 R_4 \\ & + 2\binom{\sigma}{2}\omega_2 R_2 R_7 + 4\binom{\sigma}{2}\omega_2 R_2 R_3 + 3\binom{\sigma}{2}\omega_2 R_2^2 \\ & + 2\binom{\sigma}{2}\omega_2 R_1 R_5 + 9\binom{\sigma}{3}\omega_2 R_1^2 R_2 + 6\binom{\sigma}{3}\omega_2 R_1^2 R_3 \end{aligned}$$

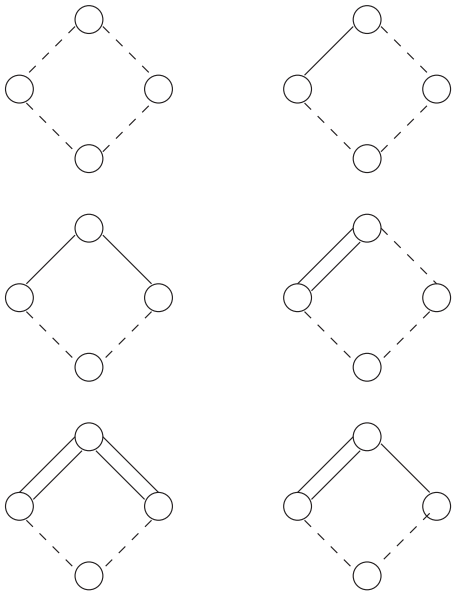

FIG. 4. Contributions to the recursion relation for the partial partition function g_0.

$$+ 6\binom{\sigma}{3}\omega_2 R_1^2 R_4 + 3\binom{\sigma}{3}\omega_2 R_1^2 R_7 + 3\binom{\sigma}{4}\omega_2 R_1^4\Bigg], \tag{2a}$$

$$B = g_0^\sigma\Bigg[\sigma\omega_1 R_1 + 6\binom{\sigma}{2}\omega_2 R_1 R_2 + 4\binom{\sigma}{2}\omega_2 R_1 R_3 + 4\binom{\sigma}{2}\omega_2 R_1 R_4 + 2\binom{\sigma}{2}\omega_2 R_1 R_7 + 3\binom{\sigma}{3}\omega_2 R_1^3 + \sigma\omega_2 R_5\Bigg], \tag{2b}$$

$$C = g_0^\sigma\Bigg[\binom{\sigma}{2}\omega_2 R_1^2 + \sigma\omega_2 R_2 + \sigma\omega_2 R_4\Bigg], \tag{2c}$$

$$D = g_0^\sigma\Bigg[\omega_1 + \binom{\sigma}{2}\omega_2 R_1^2 + \sigma\omega_2 R_2\Bigg], \tag{2d}$$

$$E = g_0^\sigma[\sigma\omega_2 R_3], \tag{2e}$$

$$F = g_0^\sigma[\sigma\omega_2 R_1], \tag{2f}$$

$$G = g_0^\sigma[\omega_2], \tag{2g}$$

$$H = g_0^\sigma[\sigma\omega_2 R_7]. \tag{2h}$$

Now we may proceed considering the operation of attaching three sets of σ subtrees to a new root square, summing all possible contributions for a fixed configuration of the bonds which are incident on the new root site. In Fig. 4 a graphical representation of the contributions to g_0' is shown to illustrate this process in the order they appear in the equation below. The recursion relations are

$$g_0' = A^3 + 2AB^2 + B^2(2C + H + D + 2E) + (2A + G)(H^2 + 2HC + 2C^2 + 4CE + 2EH) + 2BF(2C + H + 2E), \tag{3a}$$

$$g_1' = 2A^2B + 2B^3 + 2AB(2C + H + D + 2E) + 2B(2C + H + D + 2E)^2 + 2AF(2C + H + 2E) + 2FG(2C + H + 2E) + 2B(H^2 + 2HC + 2C^2 + 4CE + 2EH) + 2F(2C + H + D + 2E)(2C + H + 2E) + 4BF^2, \tag{3b}$$

$$g_2' = AB^2 + 2B^2(2C + H + D + 2E) + (2C + H)^3 + 3(2C + H)^2(D + 2E) + 3(2C + H)(D + 2E)^2 + 2BF(2C + H + 2E) + F^2G + 4F^2(2C + H) + 2F^2(D + 2E), \tag{3c}$$

$$g_3' = (D + 2E)^3 + 2F^2(D + 2E) + F^2G, \tag{3d}$$

$$g_4' = 2A^2C + 2ABF + 2B^2C + 2BF(2C + H + D + 2E) + 2ACG + 2CG^2 + 2F^2(2C + H + 2E) + 2BFG + 2C(H^2 + 2HC + 2C^2 + 4CE + 2EH), \tag{3e}$$

$$g_5' = 2H(A^2 + B^2 + AG + G^2 + H^2 + 2HC + 2C^2 + 4CE + 2EH), \tag{3f}$$

$$g_6' = 2A^2E + 2B^2E + 2AEG + 2EG^2 + 2E(H^2 + 2HC + 2C^2 + 4CE + 2EH), \tag{3g}$$

$$g_7' = 2AB(C + H + E) + 2B^2F + 2B(C + H + E)(2C + H + D + 2E) + 2BG(C + H + E) + 2F(C + H + E)(2C + H + 2E) + 2F[(2C + H)^2 + 2D(2C + H) + 4E(2C + H)] + 2FG(2C + H) + 2F^3, \tag{3h}$$

$$g_8' = 2F(D + 2E)^2 + 2FG(D + 2E) + 2FG^2 + 2F^3, \tag{3i}$$

$$g_9' = AC(C + 2E) + 2BF(C + E) + 2CG(C + 2E) + F^2(2C + H), \tag{3j}$$

$$g_{10}' = AH(2C + H + 2E) + 2BFH + 2GH(2C + H + 2E), \tag{3k}$$

$$g_{11}' = F^2(D + 2E + 2G). \tag{3l}$$

In these recursion relations the need to distinguish between the cases i and d of double bonds in the definition of the partial partition functions is apparent, for example, in the contributions to g_2': the terms proportional to C (case d) have

an additional factor of 2 as compared to the terms proportional to H (case i).

Finally, we will consider the operation of attaching $\sigma+1$ subtrees to the central site of the lattice. This operation is similar to the ones realized to obtain the recursion relations, and the result is

$$\begin{aligned} Y = g_0^{\sigma+1}\Bigg[& 1 + \binom{\sigma+1}{2}\omega_1 R_1^2 + 3\binom{\sigma+1}{4}\omega_2 R_1^4 \\ & + 9\binom{\sigma+1}{3}\omega_2 R_1^2 R_2 + 6\binom{\sigma+1}{3}\omega_2 R_1^2 R_3 \\ & + 3\binom{\sigma+1}{3}\omega_2 R_1^2 (2R_4 + R_7) + 2\binom{\sigma+1}{2}\omega_2 R_1 R_5 \\ & + (\sigma+1)\omega_1 R_2 + 3\binom{\sigma+1}{2}\omega_2 R_2^2 + 4\binom{\sigma+1}{2}\omega_2 R_2 R_3 \\ & + 2\binom{\sigma+1}{2}\omega_2 R_2 (2R_4 + R_7) + 2\binom{\sigma+1}{2}\omega_2 R_3 (2R_4 + R_7) \\ & + \binom{\sigma+1}{2}\omega_2 (2R_4^2 + R_7^2) + 2\binom{\sigma+1}{2}\omega_2 R_4 R_7 \\ & + (\sigma+1)\omega_2 (R_6 + R_8)\Bigg]. \end{aligned} \tag{4}$$

It is now easy to obtain the probabilities of single and double occupancy of the central site. The results are

$$\rho_1 = \omega_1 \frac{\binom{\sigma+1}{2} R_1^2 + (\sigma+1) R_2}{D}, \tag{5}$$

$$\rho_2 = 1 - \rho_1 - \frac{1}{D}, \tag{6}$$

where $D = Y / g_0^{\sigma+1}$.

As stated above, to study the thermodynamic behavior of the model we have to find the fixed point of the recursion relations, given the statistical weights ω_1 and ω_2. As expected, the ratios R_7 and R_8 vanish for all values of the statistical weights. On the Husimi lattice a double chain which starts on the boundary may end at any step by entering into a square and circulating it [this corresponds to the contribution $3HD^2$ in the recursion relation (3c) for g_2]. At low values of the statistical weights, a nonpolymerized (NP) phase, characterized by $\rho_1 = \rho_2 = 0$, is stable. At the fixed point associated with this phase all ratios vanish, with the exception of R_3. From the recursion relations above we may find the following equation for this fixed point:

$$(\omega_1 + 2\sigma\omega_2 R_3)^3 + [2\sigma\omega_2(1 + \omega_2 + \omega_2^2) - 1]R_3 = 0. \tag{7}$$

At the stability limit of the NP phase the largest eigenvalue of the Jacobian of the recursion relations is equal to 1 and this condition allowed us to obtain the region of the parameter space where the NP phase is stable. For large values of the statistical weights, a regular polymerized (RP) phase is stable, in which the ratios $R_1, R_2, \ldots, R_6$ are nonvanishing at the fixed point. Finally, for small values of ω_1, between the regions where the NP and RP phases are stable, a third phase appears, for which all ratios which correspond to an odd number of incoming bonds at the root site (R_1, R_5) vanish. We will call this the PP (pair polymerized) phase. In Fig. 5 the phase diagram of the model is presented for a lattice with $q=4$ and we notice that the transition between the NP and RP phases may be of first or second order, with a tricritical point located at $\omega_1 = 0.332\,551\,0(6)$ and $\omega_2 = 0.120\,544(4)$. The region where the PP phase is the most stable one is rather small, and the transition between the NP and PP phases is continuous. This transition line ends at a critical endpoint, which is located at $\omega_1 = 0.069\,560\,5(5)$ and $\omega_2 = 0.337\,074\,0(2)$. A discontinuous transition separates the two polymerized phases. The first-order lines were obtained directly from the recursion relations, starting the iterations with "natural" initial conditions [9]. In the present calculations, we considered the surface of the tree to be formed by sites connected to a single site of the next generations, as shown in Fig. 1. This choice leads to the following initial values:

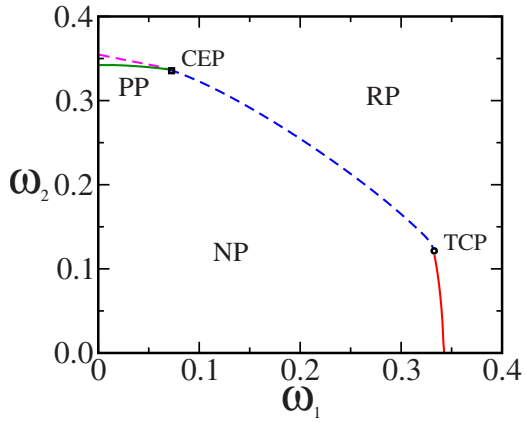

FIG. 5. (Color online) Phase diagram of the model on the Husimi lattice. Solid lines are continuous transitions and dashed lines are first-order transitions between the NP and RP (blue) phases and between the PP and RP (purple) phases. The tricritical point and the critical endpoint are also shown.

$$R_1 = 2\omega_1, \tag{8a}$$

$$R_2 = \omega_1^2, \tag{8b}$$

$$R_3 = 0, \tag{8c}$$

$$R_4 = 0, \tag{8d}$$

$$R_5 = 4\omega_1\omega_2, \tag{8e}$$

$$R_6 = 0, \tag{8f}$$

$$R_7 = 2\omega_2, \tag{8g}$$

$$R_8 = \omega_2^2. \tag{8h}$$

As mentioned above, the ratios R_7 and R_8 vanish in the thermodynamic limit, but have nonzero values for finite lattices.

If we change slightly the initial conditions, assuming the monomers placed on the surface of the tree to be distinguishable, these ratios will vanish identically and the initial value for R_4 would be equal to $2\omega_2$, with no change in the thermodynamic properties of the model within our numerical precision.

A model which is very similar to the one we are studying here was investigated recently by Zara and Pretti [16] to study the properties of RNA-like molecules, and actually the phase diagram for the Husimi lattice solution of this model is similar to the one we obtain here. It may also be mentioned that no dense phase, such as the ones found in some versions of the ISAW model [8,9], is stable in finite regions of the parameter space. Actually, such a phase is stable in a region of the $\omega_1=0$ line, but this fixed point is never reached if $\omega_1 \neq 0$ and therefore is of no physical relevance.

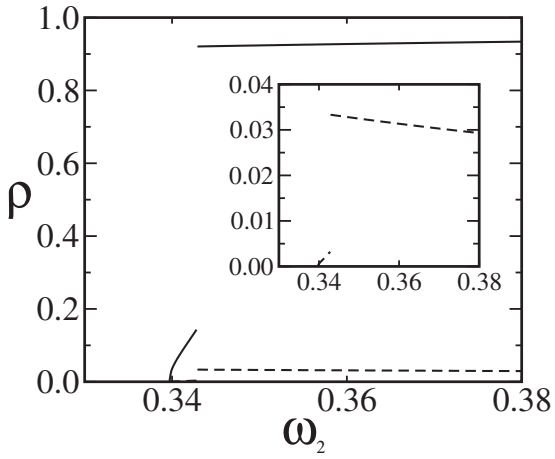

FIG. 6. Density of sites occupied by one (ρ_1, dashed lines) and two (ρ_2, solid lines) monomers, as functions of ω_2 for $\omega_1=0.05$.

III. FINAL DISCUSSIONS AND CONCLUSION

Qualitatively, the phase diagram presented here is similar to the one found for the RF model on the Bethe lattice (Fig. 3 of Ref. [14]). We notice that on the Bethe lattice the second-order line between the NP and RP phases is located at $\omega_1=1/3$, while the NP-PP transition happens at $\omega_2=1/6$ ($\omega_2=1/3$ if the monomers are considered to be indistinguishable). Those lines are no longer parallel to one of the axes for the Husimi lattice solution. The location of the tricritical point (TCP) is not changed much in the two solutions, although the value of ω_2 for this point on the Husimi lattice solution is about 10% larger. The critical endpoint (CEP), although localized at almost the same value of ω_2 in the two solutions, shows a much smaller value of ω_1 on the Husimi lattice. As a consequence, the area in which the PP phase is stable in the parameter space is much smaller on the Husimi lattice solution; it is an open question if this unusual phase appears if the model is considered on regular lattices. On the Bethe lattice solution the PP phase was called the double-occupancy polymerized phase, since ρ_1 was found to vanish in this phase. We notice that in the Husimi lattice solution the density of sites occupied by a single monomer does not vanish in this phase, as may be appreciated in the inset of Fig. 6, where both densities are shown as functions of ω_2 for a fixed value of ω_1.

Comparison of the model with multiple monomers per site (MMS) with the usual ISAW model is not straightforward. When $\omega_2=0$, the MMS model corresponds to the ISAW model without attractive interactions. However, the MMS model for $K=2$ without attractive interactions corresponds to the line $\omega_2=\omega_1^2$, since we should associate a statistical weight equal to the activity z with each monomer placed on the lattice. In the ISAW model a subset of the walks considered in the MMS model is allowed. If we actually imagine this model to be an effective description of a continuous model treated in a cell approximation, we might think the parameter ω to be the effective interaction found integrating the position of the two monomers inside the cell they occupy. If this interpretation is adopted, the statistical weight of a site occupied by one monomer would be $\omega_1=z$, where z is the activity of a monomer, while a double-occupied site would contribute with a factor ωz^2 to the grand canonical partition function, where ω is the Boltzmann factor associated with the interaction of two monomers. With this parametrization, the tricritical point will be located at $\omega \approx 1.09$, which corresponds to attractive interactions between monomers at the same site. In the Bethe lattice solution for indistinguishable monomers, the tricritical point is located at $\omega=1$, which corresponds to no interaction.

We also did the calculations of the model for distinguishable monomers, as was done initially for the Bethe lattice. Within our numerical approximation, this solution leads to a phase diagram which differs from the one presented here by a factor of 2 in the values of ω_2. This may be understood by noting that the recursion relations for the model with distinguishable monomers are the same ones presented here except for this factor of 2 in each term proportional to ω_2 for $R_1, R_2, \ldots, R_6$ (configurations 5 and 10 are absent in this case) and that the additional ratios R_7 and R_8 vanish in the fixed point for the model with indistinguishable monomers, as stated above.

ACKNOWLEDGMENTS

This work was partially financed by the Brazilian agency CNPq. P.S. acknowledges partial financial support of the Argentinian agencies SECYTUNC and CONICET, and thanks the Universidade Federal Fluminense for hospitality.

[1] P. J. Flory, *Principles of Polymer Chemistry*, 5th ed. (Cornell University Press, Ithaca, NY, 1953).
[2] S. Caracciolo, A. J. Guttmann, I. Jensen, A. Pelissetto, A. N. Rogers, and A. D. Sokal, J. Stat. Phys. **120**, 1037 (2005).
[3] P. G. de Gennes, Phys. Lett. **38A**, 339 (1972).
[4] P. G. de Gennes, *Scaling Concepts in Polymer Physics* (Cornell University Press, Ithaca, NY, 1979).
[5] J. C. Wheeler, Phys. Rev. Lett. **53**, 174 (1984); J. Chem. Phys. **81**, 3635 (1984); P. Serra and J. F. Stilck, J. Phys. A **23**, 5351 (1990); Europhys. Lett. **17**, 423 (1992); D. Maes and C. Vanderzande, Phys. Rev. A **41**, 3074 (1990).
[6] B. Derrida and H. Saleur, J. Phys. A **18**, L1075 (1985); H. Saleur, J. Stat. Phys. **45**, 419 (1986).
[7] B. Duplantier and H. Saleur, Phys. Rev. Lett. **59**, 539 (1987); B. Duplantier, Phys. Rev. A **38**, 3647 (1988).
[8] J. F. Stilck, K. D. Machado, and P. Serra, Phys. Rev. Lett. **76**, 2734 (1996); J. F. Stilck, P. Serra, and K. D. Machado, *ibid.* **89**, 169602 (2002); P. Serra, J. F. Stilck, W. L. Cavalcanti, and K. D. Machado, J. Phys. A **37**, 8811 (2004).
[9] M. Pretti, Phys. Rev. Lett. **89**, 169601 (2002).
[10] C. Buzano and M. Pretti, J. Chem. Phys. **117**, 10360 (2002).
[11] K. D. Machado, M. J. de Oliveira, and J. F. Stilck, Phys. Rev. E **64**, 051810 (2001); D. Foster, J. Phys. A **40**, 1963 (2007).
[12] M. Pretti, Phys. Rev. E **66**, 061802 (2002).
[13] J. Krawczyk, T. Prellberg, A. L. Owczarek, and A. Rechnitzer, Phys. Rev. Lett. **96**, 240603 (2006).
[14] P. Serra and J. F. Stilck, Phys. Rev. E **75**, 011130 (2007).
[15] R. Baxter, *Exactly Solved Models in Statistical Mechanics* (Academic Press, London, 1982).
[16] R. A. Zara and M. Pretti, J. Chem. Phys. **127**, 184902 (2007).